Miniband structure in $In_xGa_{1-x}As$-GaAs strained-layer superlattices

N. J. Pulsford, R. J. Nicholas, and R. J. Warburton
Clarendon Laboratory, Parks Road, Oxford OX1 3PU, United Kingdom

G. Duggan, K. J. Moore, K. Woodbridge, and C. Roberts
Philips Research Laboratories, Cross Oak Lane, Redhill RH1 5HA, United Kingdom
(Received 11 June 1990)

The miniband structure in strained $In_xGa_{1-x}As$-GaAs superlattices is studied using interband transmission and reflectivity in magnetic fields up to 16 T. Measured in-plane effective masses are in good agreement with an eight-band $\mathbf{k}\cdot\mathbf{p}$ envelope-function calculation. Significant coupling through barrier layers 100 Å thick is demonstrated by the presence of a finite miniband dispersion and a reduction in the exciton binding energy for samples with thin well layers. The superlattice Landau levels are observed to saturate in high magnetic fields near the top of the minibands, and this behavior together with the superlattice masses are fitted semiclassically using the envelope-function model. Landau levels from the $n=2$ exciton are analyzed in an uncoupled sample, and, as this state evolves into an unbound miniband, it is predicted to show very anisotropic quasi-one-dimensional behavior.

INTRODUCTION

The formation of extended miniband structure in semiconductor superlattices is a natural consequence of the imposition of a periodic layered structure on top of the crystal lattice.[1] This not only provides great practical potential for band-structure engineering, but the modeling of coupling between confined states is a valuable test of theoretical predictions.[2,3] Discrete localized quantum-well states evolve into extended Bloch-type minibands when the wave-function overlap between adjacent well layers becomes strong enough to overcome broadening due to fluctuations and collisions. Coherent electron transport through miniband Bloch states has been demonstrated by subpicosecond spectroscopy[4] and by cyclotron motion through the layers in GaAs-$Al_xGa_{1-x}As$ superlattices.[5–7]

In this paper, we study the interband optical properties of a series of strained $In_xGa_{1-x}As$-GaAs superlattices and demonstrate the presence of miniband dispersion in the growth direction for both conduction and valence bands. The effects of interwell coupling on the exciton binding energy and miniband effective masses are measured, and by using a magnetic field, we are able to characterize the change in behavior from quantum well to superlattice. An eight-band $\mathbf{k}\cdot\mathbf{p}$ envelope-function Landau-level calculation is used to model the magneto-optical results and incorporates the combined effects of strain and magnetic field on the band structure.

SAMPLE AND EXPERIMENTAL DETAILS

The superlattice samples studied were grown by molecular beam epitaxy on undoped (001) GaAs substrates.[8] The growth sequence consists of a 1-μm GaAs buffer followed by 20 periods of $In_xGa_{1-x}As$ wells and GaAs barriers and capped with a thin 200-Å layer of GaAs. All four samples have 100-Å GaAs layers, but the $In_xGa_{1-x}As$ layer thickness was varied between 25 and 200 Å with a nominal indium content of 12 at. %. X-ray measurements indicate, however, a lower indium content in the alloy layers, and a value of $\sim$9 at. % is derived from theoretical fits to the interband transition energies. The reason for the discrepancy lies in the high substrate temperature during growth (580 °C), where significant indium reevaporation occurs.[9]

As each superlattice is epitaxially lattice matched to a GaAs substrate, the $\sim$1 at. % lattice mismatch is accommodated by a tetragonal distortion of the $In_xGa_{1-x}As$ layers. X-ray studies and fits to the band-edge positions suggest that there may be some local strain relaxation in the sample with 200-Å $In_xGa_{1-x}As$ layers, but no extensive relaxation was obvious in any of the three other structures.[8] Perhaps, surprisingly, there is no significant linewidth broadening as the well thickness is increased to give a total sample thickness greater than that where some misfit dislocations begin to form. Shear strain splits the degenerate valence-band edge[10] and for a compression in the plane of the interface the heavy-hole band edge becomes higher in energy than the light-hole band edge. With a strained electron to heavy-hole offset ratio of 67:33 and using the deformation potentials suggested by Gershoni and co-workers,[11] we find for 9 at. % indium, the electrons and heavy holes are confined in the $In_xGa_{1-x}As$ layers by potential steps of 64 and 32 meV, respectively, whereas the light holes are confined in the GaAs layers by a potential barrier of only 7 meV making them a type II system with respect to the electrons. Such a type II configuration for the light holes has been clearly demonstrated by Gerard and Marzin[12] using isoelectronic substitution in each layer; however, the exact size of the confining potential, though small, is not known exactly due to uncertainties in the offset and the deformation potentials. If we compare this system to the more common-

ly studied GaAs-AlAs, we note that the confining potentials are over an order of magnitude smaller (in GaAs-AlAs,[13] they are ~1000 meV for the electrons and ~500 meV for the holes). This makes $In_xGa_{1-x}As$-GaAs an excellent candidate for studying miniband effects as strong coupling between confined states occurs for relatively thick layers of well and barrier. Not only does this avoid the problems involved with characterizing and modeling layers only a few atoms thick, but this also provides small superlattice Brillouin zones and hence measurable miniband masses for minibands as narrow as 10 meV. Furthermore, it is justifiable to use the effective-mass approximation[2] on these structures as the superlattice potential is slowly varying on the scale of the interatomic potential, with superlattice periods over 45 monolayers wide. We can use an envelope-function calculation, which includes the effects of strain on the band edges and subband effective masses,[11] to calculate the band structure: the miniband edges are plotted in Fig. 1 as the $In_xGa_{1-x}As$ thickness is varied. The four samples studied have $In_xGa_{1-x}As$ widths of 25, 50, 100, and 200 Å and are indicated by arrows along the x axis. For the thinner $In_xGa_{1-x}As$ layers, the electron and hole states are near the top of the barriers and are strongly coupled into wide minibands. As the $In_xGa_{1-x}As$ width increases, the states become more confined and the coupling is reduced, such that for 200-Å layers, the lowest states are essentially uncoupled. We should thus expect these samples to show a complete range of behavior, from isolated quantum well to strongly coupled superlattice.

The interband optical transmission and reflectivity were measured at 4.2 K in the 16-T superconducting magnet. The exciting source was chopped light from a quartz halogen lamp and Czerny-Turner monochromator, and the transmitted or reflected radiation was detected using a carbon bolometer or silicon photodiode, respectively. The magnetic field in these experiments is used to quantize the superlattice band structure. For a field perpendicular to the layers, the cyclotron motion probes just the in-plane dispersion, but if the field is orientated parallel to the layers, the field quantizes both in-plane and superlattice dispersions into Landau levels and hence allows us to map out the entire anisotropic superlattice band structure. This technique was originally used by Belle *et al.* to measure the minband width of a GaAs-$Ga_{0.6}Al_{0.4}As$ superlattice[5] and has been employed more recently to demonstrate mass anisotropy[6,14] and the effect of Γ-X mixing in GaAs-AlAs superlattices.[7]

PERPENDICULAR FIELD RESULTS— IN-PLANE DISPERSION

Figure 2 shows a series of typical transmission spectra for the 200-Å $In_xGa_{1-x}As$ well sample in different magnetic fields applied perpendicular to the layers. Excitonic features appear as clear absorption dips in the transmitted intensity. The two strong zero-field transitions at 1.415 and 1.448 eV correspond to the $E1$-hh1 and $E2$-hh2 excitons, respectively, and two weaker features are

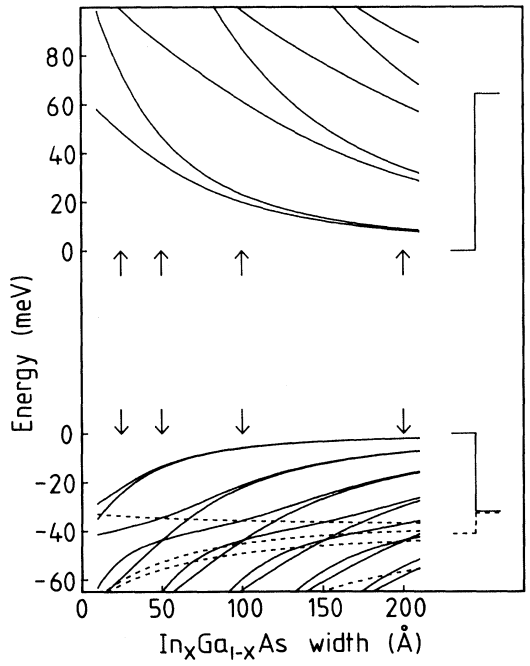

FIG. 1. Calculated superlattice miniband edges for 100-Å GaAs layers as a function of $In_xGa_{1-x}As$ thickness ($x=9\%$). The solid lines show the electrons and heavy holes which form a type I system. The dashed lines show the light holes which have type II character as indicated on the right. The arrows show the $In_xGa_{1-x}As$ thicknesses studied in this work.

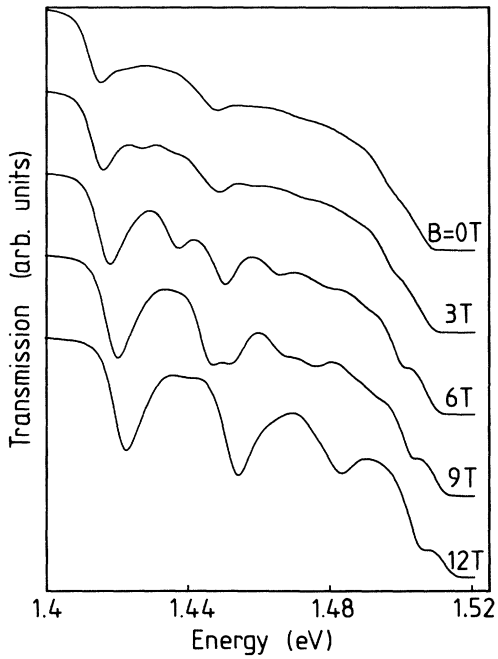

FIG. 2. Experimental traces of transmission for the 200-Å $In_xGa_{1-x}As$ sample in $B^{\perp}$. Dips in the transmission correspond to excitonic Landau-level transitions. The cutoff above 1.52 eV is due to the GaAs substrate.

present at 1.433 and 1.471 eV, which we assign to the $E1$-hh3 and $E2$-hh4 transitions. The energies of these transitions are in excellent agreement with photoluminescence excitation data on the same sample piece. No light-hole transitions are visible in this sample, which is consistent with the light holes being type II with respect to the electrons: the wave-function overlap is then very small for an essentially uncoupled system. Light-hole transitions appear, however, for the more strongly coupled samples due to the increased wave-function overlap.

In a magnetic field, Landau-level transitions are clearly visible and the energies of these levels are plotted as a function of applied field in Fig. 3. The excitonic Landau levels evolve out of the zero-field bound exciton states and one of two models can be adapted to fit the data: either a purely three-dimensional[15] (3D) or a purely two-dimensional[16] (2D) excitonic system (a superlattice exciton lies somewhere between these two extremes). The exciton binding energy and cyclotron mass are treated independently when modeling superlattice excitons to account for the anisotropic band structure. Although the 2D exciton binding energy is four times the equivalent 3D case, when the binding energies and cyclotron masses are scaled equally, the differences between these two models are relatively slight. Most notably the $1s$-$2s$ zero-field splitting is $0.75R^*$ for a 3D exciton and $0.89R^*$ for a 2D exciton, and the low-field diamagnetic shift of the $1s$ state is 25% smaller in the 2D limit. Both these differences are relatively hard to detect, leaving the binding energy as the most sensitive measure of dimensionality. This is greatest for the sample with 100-Å $In_xGa_{1-x}As$ layers where it is only two times the 3D $In_xGa_{1-x}As$ limit of $\sim$3.8 meV (see Fig. 6). We therefore use the 3D model for all samples and estimate any error thereby introduced to be less than $\sim$0.5 meV.

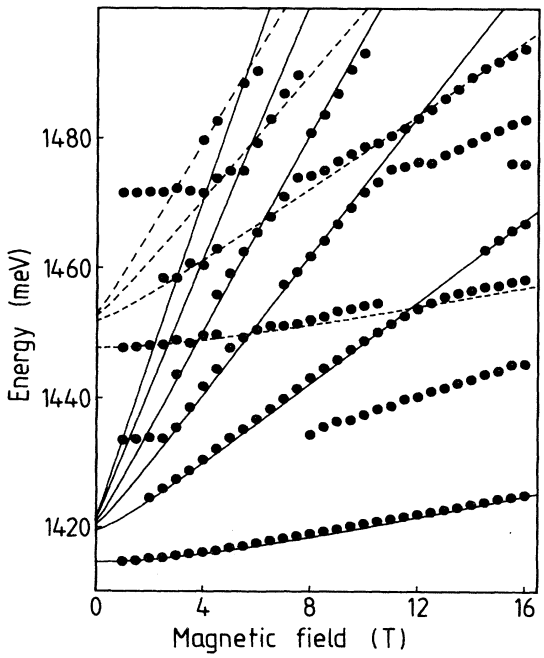

FIG. 3. Excitonic Landau-level energies as a function of perpendicular magnetic field for the 200-Å $In_xGa_{1-x}As$ sample (see Fig. 2 for spectra). The lines are modeled fits using the three-dimensional exciton model. The solid lines correspond to the $E1$-hh1 exciton and the dashed lines to the $E2$-hh2 exciton.

The fan diagram in Fig. 3 appears complicated at higher energies due to the presence of transitions crossing over each other in the spectra. However, two sets of Landau levels can be resolved, one originating from the $E1$-hh1 exciton and the other from the $E2$-hh2 exciton. The $E1$-hh1 Landau levels can be seen down to 2 T, giving an exciton binding energy of 6.5 meV. This is consistent with an enhancement over the bulk value due to confinement in a wide 200-Å well. The $E2$-hh2 exciton is fitted with a slightly smaller binding energy (5.5 meV) in line with theoretical predictions.[17] Smith and coworkers[18] have recently published reflectivity data on uncoupled 100-Å GaAs-AlAs quantum wells in which they observed Landau levels up to 8 T from both the $n=1$ and 2 excitons. They fitted their data by extending the effective-mass theory of Duggan,[19] however a considerable discrepancy was noted for the $E2$-hh2 exciton, with the measured splitting between the two lowest Landau levels being half their theoretical estimate, giving an unrealistically small exciton binding energy. Our results, however, clearly give an $E2$-hh2 binding energy (from the $n=1$ Landau level at low fields) which is intermediate between the bulk, 3D value and the strongly confined $E1$-hh1 exciton and this is probably due to the finite bandwidth (4 meV) of the $n=2$ electron subband. The fit to the $1s$ diamagnetic shift is about 15% too small. The reason for the discrepancy in the model is probably that the shape of a hydrogenic magnetoexciton is a much better approximation to an $n=1$ than an $n=2$ exciton, particularly in that an $n=2$ exciton has a broader spatial extent giving the greater shift. Unfortunately, the calculations of Smith for an $n=2$ exciton are only valid for modest fields (Duggan estimates 0–4 T) and so it is not possible to make a valid comparison with high-field data up to 15 T.

In the three narrower well samples, higher excitonic Landau levels are only observed originating from the $E1$-hh1 transition. These are plotted as a function of magnetic field for the 25-Å $In_xGa_{1-x}As$ sample in Fig. 4. In zero field, there are two sharp absorption features at 1.493 and 1.500 eV, which correspond to the $E1$-hh1 and $E1$-lh1 excitons. As these lie only $\sim$20 meV below the bulk GaAs band edge, the reflectivity rather than transmission is measured, allowing the band structure above the top of the GaAs barriers to be investigated. The reflectivity line shapes are modeled by taking a Lorentzian dielectric response for the excitons[20] and using a transfer-matrix technique to account for the layered structure. In contrast to previous studies on GaAs-AlAs, where the line shape was found to be asymmetric both experimentally and theoretically, the line shape in these samples is very similar in form to the transmission: a sharp dip in the reflected intensity occurs at the transition position. The lack of strong asymmetry is probably due to the short optical path across the capping layer[20]

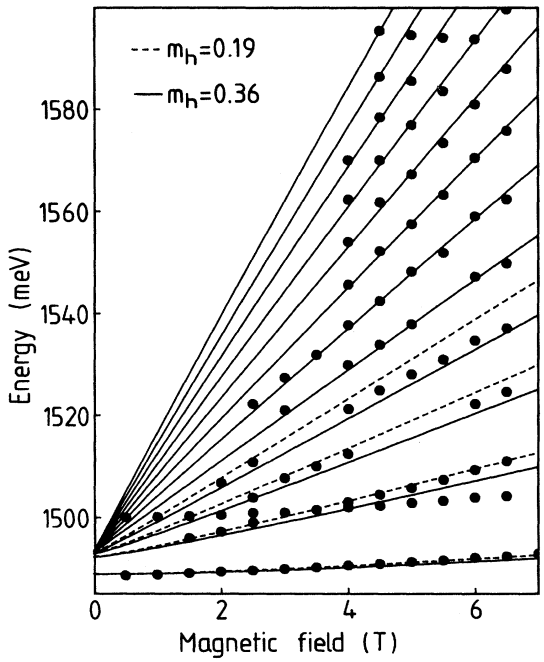

FIG. 4. Excitonic Landau levels for the 25-Å $In_xGa_{1-x}As$ sample in $B^{\perp}$. Reflectivity is used to measure above the GaAs band edge. The solid lines show fits using a "heavy-"hole mass of $0.36m_0$, which is appropriate at high energies once the valence bands are strongly mixed. At low energies, a lighter decoupled hole mass of $0.19m_0$ gives a better fit (dashed lines).

($\sim\gamma/10$) and a weak modulation of the real part of the refractive index by the layered superlattice. This minimizes interference effects near the surface so that the changes in reflectivity are dominated by the imaginary part of the refractive index, i.e., the absorption.

The gap in the fan diagram (Fig. 4) in the energy range 1.515–1.520 eV is where the bulk GaAs 1s exciton dominates the spectrum. Above the GaAs band edge, two sets of Landau levels are observed, one originating from bulk GaAs and the other from the superlattice. The bulk Landau levels are visible for low fields (2–4 T), producing a modulation of the reflectivity of $\sim 0.5\%$, but as the field increases, stronger superlattice levels start to pass through such that above 6 T it is no longer possible to identify bulk levels. The reason for the dominance of the superlattice levels is the thin capping layer: the greatest change in refractive index occurs at the air interface and the short optical path across the capping layer makes it optically translucent to the incoming radiation. Only transitions originating from the superlattice are plotted in Fig. 4, and these are fitted using the 3D exciton model (solid lines). The binding energy (4.5 meV) is determined from low-field extrapolation of the $n=1$ level down to 1.5 T. A heavy-hole mass of $0.19m_0$ (dashed lines) is required to fit the levels at low energies, but this gives a poor fit above about 1.54 eV. At higher energies, even taking into account the effect of the electron subband nonparabolicity, a much heavier hole mass of $0.36m_0$ is required (solid lines), indicating that the valence-band

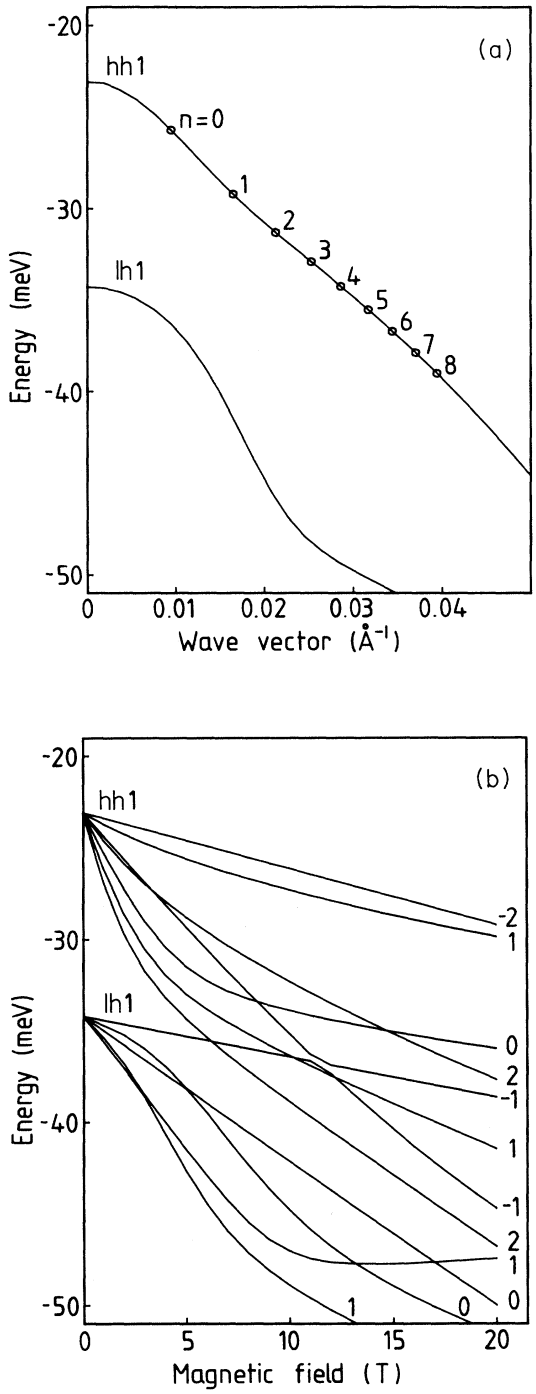

FIG. 5. (a) Six-band $\mathbf{k}\cdot\mathbf{p}$ envelope-function calculation of the valence in-plane dispersion for the 25-Å sample in zero magnetic field. The interaction between the hh1 and lh1 subbands mixes the character and increases the hh1 mass away from $k_{\parallel}=0$. The open circles indicate the radii of the semiclassical cyclotron orbits observed experimentally in 6 T and are labeled with the Landau index n. (b) Eight band $\mathbf{k}\cdot\mathbf{p}$ envelope-function calculation of the valence-band Landau-level structure for the 25-Å $In_xGa_{1-x}As$ sample. The quantum numbers $-2,-1,-0,\ldots$, follow the standard notation (see, for example, Ref. 21).

TABLE I. Variation of high field value hh1 effective mass with energy separation of heavy- and light-hole subbands.

$d_{In_xGa_{1-x}As}$ (Å)	E_{hh}-E_{lh} (meV)	m_{hh}
25	12	0.36
50	26	0.25
100	32	0.23
200	34	0.19

structure is very nonparabolic. Such behavior is well known and arises from the mixing of heavy- and light-hole states away from $k_{\|}=0$.[21] In GaAs-$Al_xGa_{1-x}As$ quantum wells, similar behavior has been observed at very low magnetic fields;[22] however, in strained $In_xGa_{1-x}As$-GaAs structures, the heavy- and light-hole splitting is much greater and a decoupled (unmixed) mass can be observed over a wider range of energy (or field). Indeed, cyclotron resonance on a *p*-type sample with 14 at. % indium content has measured a mass of $0.155m_0$ close to $k_{\|}=0$ for the hh1 band[23] indicating the decoupled nature. A calculation of the valence-band structure and corresponding Landau levels for the 25-Å sample using six- and eight-band $\mathbf{k}\cdot\mathbf{p}$ envelope-function models, respectively, are shown in Figs. 5(a) and 5(b). In the in-plane dispersion, the increase in hole mass is due to the interaction between the hh1 and lh1 states away from $k_{\|}=0$. The radii of the semiclassical orbits in k space for the nine Landau levels observed experimentally in 6 T (Fig. 4) are indicted in Fig. 5(a) and clearly sample both the light and heavy values of the hh1 mass. The calculated interband transition energies using the Landau levels in Fig. 5(b) and an analogous set for the conduction band agree well with the experimental results over the whole field range used.

There is a clear trend of decreasing high-energy hh1 mass with increasing $In_xGa_{1-x}As$ width over the four samples (see Table I). The linewidths in the 50- and 100-Å samples are not so sharp as the 25-Å sample, and it is not possible to see strong nonparabolicities due to the uncoupled mass at low fields. However, the decrease in mass at large $k_{\|}$ fits in with a progressive decoupling of the hh1 and lh1 subbands as their separation increases.

PARALLEL FIELD RESULTS— INTERWELL COUPLING

The exciton binding energy in a semiconductor superlattice is a very sensitive measure of the exciton dimensionality and hence also of the lateral extent of the excitonic wave function. In the two-dimensional limit, it is enhanced by a factor of 4 over its three-dimensional value. Hence the binding energy in a 22-Å GaAs-$Al_xGa_{1-x}As$ quantum well has been measured to be 13 ± 3 meV,[24] which compares with a bulk GaAs band-edge value of 4.2 meV (Ref. 25) (though part of the enhancement is due to band nonparabolicities). The measured binding energies of the four samples are shown in Fig. 6 (solid circles) as a function of $In_xGa_{1-x}As$ width together with the bulk GaAs value, which corresponds to the zero thickness limit. Also shown (open squares) are some binding energies measured by photoluminescence excitation spectroscopy in samples with much thicker barrier layers.[26] These are effectively uncoupled wells and the energies show good agreement with calculations for an isolated well (solid line). In contrast, the exciton binding energies in the strongly coupled samples lie substantially below the isolated well values. For 25 Å, the energy of 4.5 meV is little more than that of bulk GaAs, consistent with the structure acting as a weakly anisotropic three-dimensional solid. The binding energy then increases rapidly towards the iolated well value as the states become more confined into the well layers. For wider $In_xGa_{1-x}As$ layers, the exciton spreads out within the well leading to a gradual decrease in the binding energy towards the three-dimensional limit (estimated value for bulk $In_xGa_{1-x}As$ is ~3.8 meV). The peak in the exciton binding energy at the 100-Å sample indicates the strong effect of coupling in these structures for even relatively thick layers. For the isolated wells the confinement is stronger leading to a peak binding energy for much narrower wells, around 50 Å.

A more definitive demonstration of electronic coupling in a superlattice is the presence of a finite miniband dispersion in the growth direction. This may be probed by orientating the magnetic field parallel to the sample layers so that the cyclotron orbits involve both in-plane and superlattice motion. Landau levels are only observed if there are extended Bloch states through the superlat-

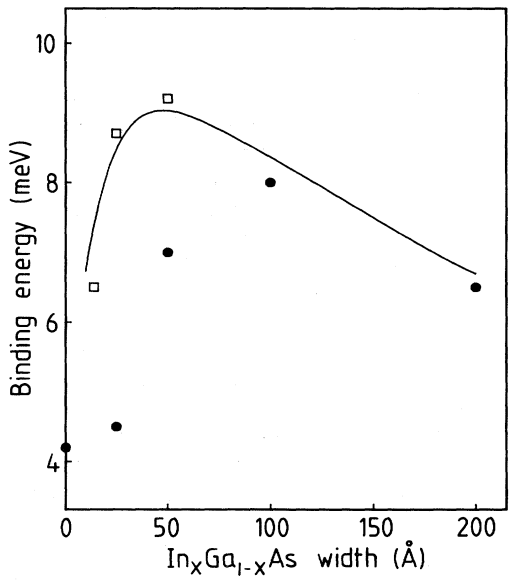

FIG. 6. Solid circles show the measured $E1$-hh1 exciton binding energy as a function of $In_xGa_{1-x}As$ well thickness in these samples. The open squares and solid line are taken from Ref. 26 and show the measured and calculated binding energy in isolated well samples. The difference between the two sets of data for thin wells illustrates the effect of interwell coupling on the binding energy in this region.

tice and the corresponding Landau-level separation is now smaller due to the heavier cyclotron mass.[6] Figure 7 shows the experimentally measured Landau levels in the 25-Å $In_xGa_{1-x}As$ sample. An envelope-function calculation predicts miniband widths of 20.3 and 1.6 meV for the electron and heavy-hole minibands, respectively, so any structure associated with the top of the electron miniband is not visible due to the dominance of the GaAs $1s$ exciton in that part of the spectrum. In contrast to $B^{\perp}$, no superlattice levels are seen above the GaAs exciton, indicating a finite superlattice miniband width which is less than ~ 30 meV wide. However, levels below 1.510 eV are visible and these are fitted using the 3D exciton model. The cyclotron mass is calculated by taking a geometric average of the in-plane and superlattice masses for each particle and then taking the usual reduced mass. The in-plane masses and binding energy are then taken from the perpendicular field data and the superlattice masses are calculated using an envelope-function calculation. The fit is good at low energies and confirms the calculated reduced mass anisotropy of $\mu^{\perp}/\mu^{\parallel}=1.29$. However, the fit at higher energies is poor, considerably overestimating the transition energies even when the electron miniband nonparabolicity is taken into account (dashed line). The reason for this discrepancy is due to the heavy-hole miniband saturating.

The heavy-hole miniband is narrow due to the heavy tunneling mass in the growth direction and, when combined with the light decoupled in-plane mass ($0.19m_0$), the superlattice Landau levels reach the top of the heavy-hole miniband well before the top of the electron miniband. The saturation of the hole miniband reduces the cyclotron energy increase—the low-energy gradient is due to the combined electron-hole reduced mass, whereas the gradient at higher energies is just due to the electron mass alone. From the miniband width, we can estimate semiclassically the "fundamental" field at which the $n=0$ heavy-hole Landau level reaches the miniband top to be 13.8 T; hence the $n=1$ and 2 levels are predicted to saturate at 4.6 and 2.8 T, respectively, and these are indicated by arrows in Fig. 7. In their original experiments, Belle and Maan[5] found that no sharp parallel field Landau levels are observed when the miniband width is exceeded. Indeed, any discrete levels above the top of the miniband are not possible in a semiclassical picture as they lead to open orbits which cannot satisfy the usual quantization conditions.[27] Mann's calculation[3] showed that for levels both near the top and above the miniband, the Landau-level energy depends on the orbit position (in real space) which makes transitions very broad and weak. This does not happen for the holes in this case due to the narrow-hole miniband width (1.6 meV), though it remains unclear exactly which hole states are combining with the discrete electron Landau levels. Intuitively, however, the mass gets very heavy near the top of the miniband and the solid lines in Fig. 7 are calculated using a semiclassical quantization of both the electron and hole band structures assuming no further increase in energy once the miniband top is reached. The data fit much better with the change in gradient at fields where the heavy holes saturate (indicated by arrows). Berezhkovskii and Suris[28] have shown that strong fields (about twice the saturation field) localize the extended miniband states into single wells, i.e., actually change the band structure. As Maan pointed out, the crucial assumption of a semiclassical approach is that the magnetic field does not alter the band structure but only allows certain values of energy in the existing band structure. However, Maan also showed that within the miniband, a semiclassical quantization gives essentially the same results as a full calculation involving electrical and magnetic quantization together, and the use of a semiclassical model not only gives a clearer picture but allows the inclusion of exciton effects which are important at low fields.

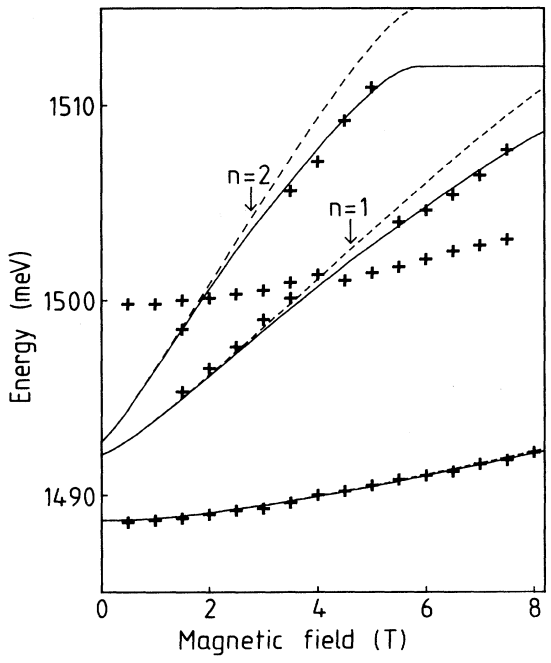

FIG. 7. Excitonic Landau levels for the 25-Å $In_xGa_{1-x}As$ sample in the parallel field orientation. No levels are observed above the range of the bulk GaAs exciton (1.51–1.52 eV), indicating the finite minband width in this sample. The solid lines show fits including the full miniband structure, while the dashed lines assume a constant hole mass. The arrows indicate the change in gradient due to the hole miniband saturating.

We now turn our attention to the 50-Å $In_xGa_{1-x}As$ sample where the coupling and hence the miniband widths are reduced. The Landau-level diagrams for $B^{\perp}$ and $B^{\parallel}$ are shown in Figs. 8 and 9. In the experimental spectra, there are two distinct contributions to the $E1$-hh1 exciton transmission line shape at zero field, though the lower-energy feature gradually dominates as the field is increased. The presence of multiple lines in the luminescence of these and other samples indicates indium fluctuations across the superlattice which localize the heavy-hole states into a few well layers.[8] The hole states are particularly sensitive to localization effects because of their narrow bandwidth. This interpretation is supported by the reflectivity on the same sample piece which picks out the lower-energy feature much more strongly; the

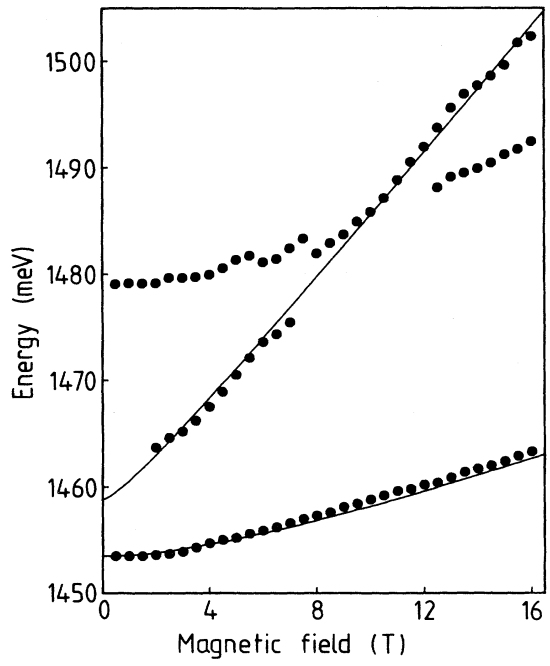

FIG. 8. Excitonic Landau levels for the 50-Å $In_xGa_{1-x}As$ sample in $B^{\perp}$. The zero-field transitions at 1.454 and 1.480 eV are the $E1$-hh1 and $E1$-lh1 excitons, respectively.

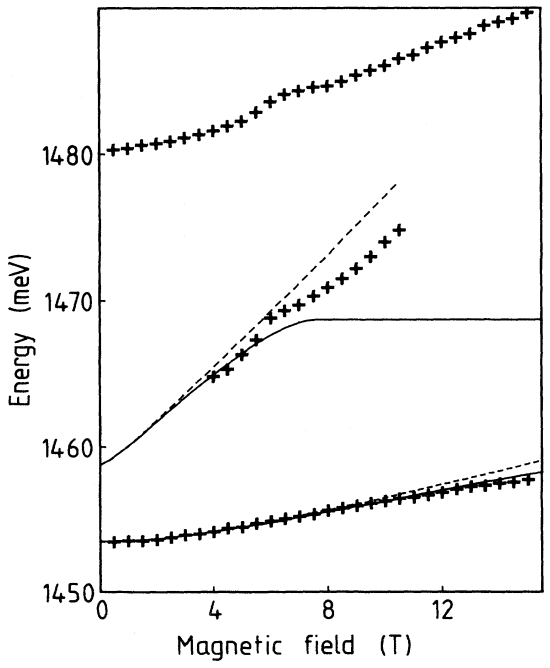

FIG. 9. Excitonic Landau levels for the 50-Å $In_xGa_{1-x}As$ sample in the parallel field orientation. The solid lines are calculated using a semiclassical quantization of the full band structure, while the dashed lines assume a constant electron mass and hence ignore the effect of the miniband gap.

reflectivity is more heavily influenced by the top layers near the air interface (presumably where the lower-energy exciton is localized) compared with the transmission, which takes a more even average throughout the whole structure. In addition, in the 25-Å $In_xGa_{1-x}As$ sample, about 3 meV below the main $E1$-hh1 feature, there is a weaker transition which has a 15% smaller $B^{\parallel}$ diamagnetic shift indicating a more tightly localized exciton. The presence of two lines in the 50-Å $In_xGa_{1-x}As$ sample coupled with the increase in linewidth due to alloy broadening ($\sim$4 meV) allows only the lowest two excitonic Landau levels ($1s$ and $2p$) to be observed. This is sufficient though to obtain a value for the exciton binding energy (7 meV) and the in-plane hole mass ($0.25m_0$). In the parallel magnetic field orientation (Fig. 9), again two $E1$-hh1 exciton levels are observed allowing a calculated value of 1.56 for the band-edge reduced mass anisotropy ($\mu^{\perp}/\mu^{\parallel}$) to be confirmed. The $n=1$ Landau level weakens and dies out around 10 T, which appears consistent with a finite miniband width. However, a semiclassical quantization of the band structure considerably underestimates the energy at which the saturation occurs even if the GaAs barriers are reduced to 90 Å (solid lines), giving miniband widths of 13 and 0.5 meV for the electrons and heavy holes, respectively. In contrast, the fit for the $1s$ shift is good, indicating that the miniband masses and hence widths are fairly accurate. One possible reason for the discrepancy is that the enhanced magnetoexciton binding energy is being overestimated near the top of the miniband where the differential mass is negative. This is unlikely, as reducing the binding energy would just increase the slope of the excitonic line and not extend it as is required. Instead, we attribute this behavior to the superlattice miniband structure breaking down. This may be due either to imperfections in the superlattice periodicity due to fluctuations in indium content[8] (the linewidth $\sim$5 meV is at its widest in this sample), weakening the q quantum number conservation rule, or possibly due to the miniband width and exciton binding energy being of a similar size and hence modifying the magneto-band-structure.[29] The dashed line in Fig. 9 is calculated using a constant electron mass (i.e., ignoring the superlattice miniband gap) and the experimental points lie intermediate between the two limits.

No higher excitonic Landau levels are observed in the parallel field configuration for the two weakly coupled samples with 100- and 200-Å $In_xGa_{1-x}As$ layers. However, it is possible to trace the complete change in exciton behavior from superlattice to quantum well by comparing the diamagnetic shifts of the $E1$-hh1 $1s$ exciton states. In a perpendicular field [Fig. 10(a)], the shifts for all four samples are similar, reflecting the relatively weak dependence of the high-field diamagnetic shift on the exciton binding energy (the reduced masses do not vary much). In a parallel magnetic field [Fig. 10(b)], the variation is much greater. There is a rapid decrease in shift as the coupling is reduced and the exciton becomes confined to a single well. The shape of the curve also changes from being subparabolic, almost linear, which is characteristic of a three-dimensional exciton, to a purely parabolic shift which is characteristic of an isolated quantum well.[30]

The increase in shift for the wide 200-Å $In_xGa_{1-x}As$ sample is due to the exciton spreading out in the well and regaining some of its three-dimensional character. The parabolic shifts are modeled by using a perturbation approach on the envelope functions,[30] where

$$V_p = \frac{e^2B^2z_e^2}{2m_e^{\parallel}} + \frac{e^2B^2z_h^2}{2m_h^{\parallel}}$$

is the perturbing potential and $m_e^{\parallel}$ and $m_h^{\parallel}$ are the in-plane effective masses. Both the first- and second-order shifts are calculated, but even at 16 T, the quartic second-order shift is typically only $\sim 10\%$ of the quadratic first-order shift. For the 200-Å well sample, a hydrogenic excitonic envelope with a Bohr radius of 150 Å is included on top of the envelope functions to mimic the additional confining effect of the Coulomb potential and this reduces the calculated shift by about 15%. As with previous parallel field studies, the exciton binding energy is taken to be independent of the magnetic field.[30,31] Using the in-plane effective masses from the perpendicular field Landau-level fits, the calculated diamagnetic shifts are in good agreement with the experimental data.

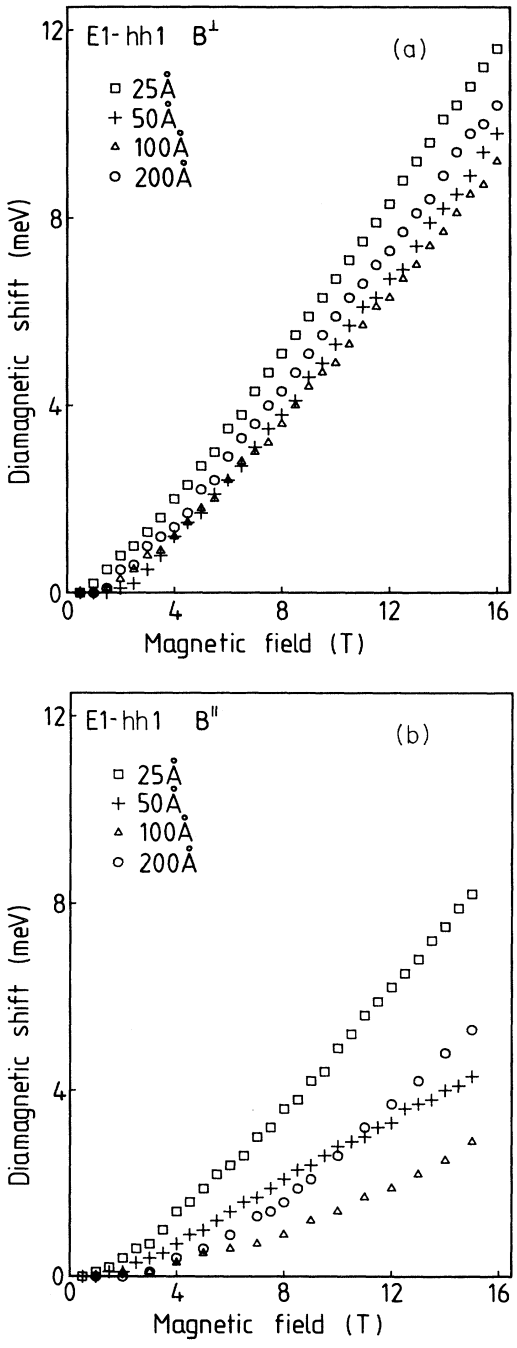

FIG. 10. (a) Diamagnetic shifts of the $E1$-hh1 exciton for the four different samples in $B^{\perp}$. (b) Diamagnetic shifts in $B^{\parallel}$. The shift becomes strongly parabolic for the uncoupled samples.

The shift of the $n=2$ exciton in the 200-Å $In_xGa_{1-x}As$ is $\sim 60\%$ larger in the parallel field than in the perpendicular field orientation. This is expected as the state evolves into an $n=1$ Landau level in the limit of a very strong magnetic field.[32] It is interesting to study this behavior when the $n=2$ level evolves from being an uncoupled quantum-well state to an unbound miniband. In the 25-Å $In_xGa_{1-x}As$ sample (most strongly coupled), the lowest two electron miniband widths are 20.3 and 68.8 meV, respectively, separated by a miniband gap of 25.3 meV. In the nearly-free-electron approximation, the band-edge mass is inversely proportional to the band gap and a similar argument applies to minbands leading to very light superlattice masses for the higher bands. In this case, an envelope-function calculation predicts an $n=2$ band-edge mass of $0.003m_0$ in the growth direction, which rises to a value of $0.005m_0$ at 10 meV into the miniband. This represents an inverted mass anisotropy of about 20, which is much larger than the mass anisotropy measured in the $n=1$ minibands and should lead to the formation of a very anisotropic prolate exciton, which is quasi-one-dimensional. A decrease in the binding energy due to the change in effective mass is expected, but much more striking would be the Landau-level separation in $B^{\parallel}$, increased by about a factor of 4 over the $B^{\perp}$ behavior. Unfortunately, no modulation of the reflectivity is visible around the $n=2$ exciton position in this sample; the reason probably being that only 20 superlattice periods are not enough to form a true miniband, which is 70 meV wide. However, a measurement of the $n=2$ miniband mass would provide an elegant demonstration of the effect of the periodic superlattice potential and is the basis of a present study in this system.

SUMMARY

In conclusion, we have studied the formation of minibands in strained $In_xGa_{1-x}As$-GaAs superlattices as the coupling between confined states is increased. This leads to a decrease in the exciton binding energy and the formation of a finite miniband dispersion and miniband mass. A magnetic field is used to measure the superlattice band structure and the effects of strain and interwell coupling on the subbands are demonstrated. The resulting masses, both in-plane and superlattice, are in good agreement with an eight-band $\mathbf{k}\cdot\mathbf{p}$ envelope-function cal-

culation. However, such good agreement is not always found with the saturation of the minibands due to their finite energy width, and this is thought to be either due to inhomogeneity in the superlattice structure or to a failure of the semiclassical model for narrow miniband widths. The $n=2$ exciton is studied in an uncoupled sample and this is predicted to become very anisotropic as the coupling is increased.

[1]L. Esaki and R. Tsu, IBM J. Res. Dev. **14**, 61 (1970).
[2]G. Bastard, Acta Electron. **25**, 147 (1983).
[3]J. C. Maan, Festkörperprobleme **27**, 137 (1987).
[4]B. Deveaud, J. Shah, T. C. Damen, B. Lambert, and A. Regreny, Phys. Rev. Lett. **58**, 2582 (1987).
[5]G. Belle, J. C. Maan, and G. Weimann, Solid State Commun. **56**, 65 (1985).
[6]T. Duffield, R. Bhat, M. Koza, F. DeRosa, D. M. Huang, P. Grabbe, and S. J. Allen, Phys. Rev. Lett. **56**, 2724 (1986).
[7]N. J. Pulsford, R. J. Nicholas, P. Dawson, K. J. Moore, G. Duggan, and C. T. Foxon, Phys. Rev. Lett. **63**, 2284 (1989).
[8]K. J. Moore, G. Duggan, K. Woodbridge, and C. Roberts, Phys. Rev. B **41**, 1095 (1990).
[9]C. T. Foxon and B. A. Joyce, J. Cryst. Growth **44**, 75 (1978).
[10]C. G. Van der Walle, Phys. Rev. B **39**, 1871 (1989).
[11]D. Gershoni, H. Temkin, M. B. Panish, and R. A. Hamm, Phys. Rev. B **39**, 5531 (1989).
[12]J. M. Gerard and J. Y. Marzin, Phys. Rev. B **40**, 6450 (1989).
[13]K. J. Moore, P. Dawson, and C. T. Foxon, Phys. Rev. B **38**, 3368 (1988).
[14]N. J. Pulsford, R. J. Nicholas, P. Dawson, K. J. Moore, and C. T. Foxon, Superlatt. Microstruct. **6**, 51 (1989).
[15]P. C. Makado and N. C. McGill, J. Phys. C **19**, 873 (1986).
[16]O. Akimoto and H. Hasegawa, J. Phys. Soc. Jpn. **22**, 181 (1967).
[17]J. A. Brum and G. Bastard, J. Phys. C **18**, L789 (1985).
[18]D. D. Smith, M. Dutta, X. C. Liu, A. F. Terzis, A. Petrou, M. W. Cole, and P. G. Newman, Phys. Rev. B **40**, 1407 (1989).
[19]G. Duggan, Phys. Rev. B **37**, 2759 (1988).
[20]P. C. Klipstein and N. Apsley, J. Phys. C **19**, 6461 (1986).
[21]A. Fasolino and M. Altarelli, in *Two Dimensional Systems, Heterostructures and Superlattices*, Vol. 53 of *Solid State Science*, edited by G. Bauer, F. Kuchar, and H. Heinrich (Springer-Verlag, Berlin, 1984), p. 176.
[22]A. S. Plaut, J. Singleton, R. J. Nicholas, R. T. Harley, S. R. Andrews, and C. T. Foxon, Phys. Rev. B **38**, 1323 (1988).
[23]D. Lancefield, W. Batty, C. B. Crookes, E. P. O'Reilly, A. R. Adams, K. P. Homewood, G. Sundaram, R. J. Nicholas, M. Emeny, and C. R. Whitehouse, Surf. Sci. **229**, 122 (1990).
[24]D. C. Rogers, J. Singleton, R. J. Nicholas, C. T. Foxon, and K. Woodbridge, Phys. Rev. B **34**, 4002 (1986).
[25]D. D. Sell, Phys. Rev. B **6**, 3750 (1972).
[26]K. J. Moore, G. Duggan, K. Woodbridge and C. Roberts, Phys. Rev. B **41**, 1090 (1990).
[27]G. E. Zil'berman, Zh. Eksp. Teor. Fiz. **33**, 387 (1958) [Sov. Phys.—JETP **6**, 299 (1958)].
[28]A. M. Berezhkovskii and R. A. Suris, Zh. Eksp. Teor. Fiz. **86**, 193 (1984) [Sov. Phys.—JETP **59**, 109 (1984)].
[29]The theory is from H. Chu and Y-C. Chang, Phys. Rev. B **36**, 2946 (1987); experimental results are from K. J. Moore, G. Duggan, A. Rakemura, and K. Woodbridge, Phys. Rev. B **42**, 1326 (1990).
[30]N. J. Pulsford, J. Singleton, R. J. Nicholas, and C. T. Foxon, J. Phys. (Paris) Colloq. **48**, C5-231 (1987).
[31]W. Ossau, B. Jäkel, E. Bangert, G. Landwehr, and G. Weimann, Surf. Sci. **174**, 188 (1986).
[32]W. Zawadzki, Semicond. Sci. Technol. **2**, 550 (1987).